Shahid Chamran University of Ahvaz

Irrigation Sciences and Engineering (JISE)
Vol. 45, No. 2, Summer 2022, p. 1-18

Original Paper

Journal homepage: https://jise.scu.ac.ir

Development of a Multi-Aspects Groundwater Vulnerability Index in the Transboundary Aquifer between Syria, Iraq, and Turkey in light of the water conflict and climate change

M. Al-Mohamed[1], A. Sotoodehnia[2*], P. Daneshkar Arasteh[3] ,N. Al-Ansari[4], A. Azizian[5] and H. Ramezani Etedali[6]

1- Water Engineering Department, Faculty of Agriculture and Natural Resources, Imam Khomeini International University, Qazvin, Iran and Environmental Engineering Technologies Department, Faculty of Technical Engineering, Aleppo University, Aleppo, Syria.
2- Corresponding Author, Water Engineering Department, Faculty of Agriculture and Natural Resources, Imam Khomeini International University, Qazvin, Iran . (sotoodehnia@eng.ikiu.ac.ir).*
3- Water Engineering Department, Faculty of Agriculture and Natural Resources, Imam Khomeini International University, Qazvin, Iran.
4- Civil, Environmental and Natural Resources Engineering Department, Lulea University of Technology, Lulea, Sweden.
5- Water Engineering Department, Faculty of Agriculture and Natural Resources, Imam Khomeini International University, Qazvin, Iran.
6- Water Engineering Department, Faculty of Agriculture and Natural Resources, Imam Khomeini International University, Qazvin, Iran.

ARTICLE INFO

Artlcle history:
Received: 19 May 2022
Revised: 11 June 2022
Accepted: 13 June 2022

Keywords:
Groundwater, Transboundary, Vulnerability, Syria, Composite Index.

TO CITE THIS ARTICLE:

Al-Mohamed, M., Sotoodehnia, A., Daneshkar Arasteh, P., Al-Ansari, N., Azizian, A., Ramezani Etedali, H. (2022). 'Development of a Multi-Aspects Groundwater Vulnerability Index in the Transboundary Aquifer between Syria, Iraq, and Turkey in light of the water conflict and climate change', Irrigation Sciences and Engineering, 45(2), pp. 1-18.

Abstract

Groundwater vulnerability assessment is an effective tool in the joint management of transboundary groundwater, especially in developing countries where data is scarce, monitoring networks are insufficient, and water is both a cause and a target of conflicts. The Jezira Tertiary Limestone Aquifer Transboundary System (JTLATS) region, which Syria, Iraq, and Turkey share, gives a clear description of the shared water problem in developing countries with arid and semiarid environments. In this study, a comprehensive multidisciplinary Groundwater Vulnerability Index (GVI) was developed as a distributed composite index to assess the groundwater vulnerability in JTLATS by combining different environmental and political socioeconomic datasets and models for three periods between 2003 and 2017. The JTLATS was categorized into five zones: very low, low, moderate, high, and very high vulnerability. The results showed a low vulnerability in the southern regions of the aquifer. In comparison, the areas with high vulnerability are primarily spread in the northern and western parts of the JTLATS and along the Euphrates river. The results showed an increase in the percentage of areas with high vulnerability from 10.45% in (2003-2007) to 13.42% and 20.57% of the aquifer area in (2007-2011) and (2011-2017), respectively. The groundwater vulnerability in the aquifer increased with the spread of political instability in both Syria and Iraq and the increase in cultivated areas in Turkey

Introduction

Water has been included as one of the United Nations Sustainable Development Goals adopted in 2015. Target 6 is dedicated to clean water and sanitation, including groundwater. Objective 6.5 calls for implementing integrated water resources

management at a transboundary level when needed (Mccracken, 2017). Transboundary surface waters have been extensively studied worldwide, while transboundary groundwater has received less attention (Rivera and Candela, 2018). Currently, 592 transboundary groundwater aquifers worldwide, 226 of which are groundwater bodies defined under the EU Water Framework Directive (IGRAC, U. I, 2015). The transboundary aquifers were studied in light of the need for their management and the conclusion of agreements between the riparian countries. In this Context, Fraser et al. (2020) have identified transboundary aquifers in Malawi at risk of over-abstraction or reduced water quality (hotspots). They pinpointed specific areas in the country that may be at transboundary risk using fuzzy logic and GIS overlay.

Groundwater is an essential source of water that meets the various needs in the Middle East. This importance is due to the limited surface water resources, droughts, and the spread of wars in the region. The Jezira Tertiary Limestone Aquifer Transboundary System (JTLATS) region, which extends between Syria, Turkey, and Iraq, has a long history of political and social instability and conflict over water resources. JTLATS region is also characterized as a food basket for Syria, where about 60% of the irrigated lands are concentrated (Allan et al., 2012),

UN-ESCWA (2013) studied the JTLATS within the "Inventory of Shared Water Resources in West Asia". This study provided information about the climate, population, and hydrogeology of the JTLATS. International Groundwater Resources Assessment Center (IGRAC, 2015) has also restricted the JTLATS boundaries based on the study of UN-ESCWA (2013).

Several studies have been conducted within the JTLATS region. These studies were either on minor aquifers on a local scale that dealt with the hydrochemical characteristics of groundwater or on a regional scale that dealt with the groundwater depletion in the Tigris and Euphrates rivers basin, of which the JTLATS forms a part.

On the local scale, Kattan (2018) used hydrochemical and environmental isotope methods to characterize the Euphrates alluvial aquifer's groundwater quality in Syria. He concluded that the salinity of groundwater gradually increased from north to south, changing from almost freshwater near the Syrian–Turkish border to brackish water in the vicinity of Al-Raqqa. In Turkey, Yesilnacar and Gulluoglu (2008) studied the effect of surface irrigation as a result of operating the GAP project on groundwater quality in the Harran Plain. They showed that EC and nitrate values measured were considerably above the guide level.

As for studies on a regional scale, Lezzaik et al. (2018) built a composite groundwater risk index (taken in depletion terms only) within the MENA region, considering the hydrogeological and socioeconomic aspects. The results of this index indicated a strong dependency of groundwater risk on governance and food security factors. Despite this progress, no studies have been conducted to assess the groundwater vulnerability to pollution on a regional scale in the JTLATS. Many methods are used to study the groundwater vulnerability, such as DRASTIC, COP, SINTACS, RISKE, and EPIK (Barbulescu 2020; Ghadimi et al. 2022; Taghavi et al. 2022). Not only the environmental and hydrogeological conditions that control the choice of the method used, but also the lack of available data has a significant role in that, as is the case in the JTLATS. Large-scale groundwater vulnerability assessment is critical and practical for designing groundwater management and protection strategies. In this context, Ouedraogo et al. (2016) assessed the African scale's intrinsic vulnerability and risk of groundwater pollution. They deployed the empirical index model DRASTIC into a GIS to assess the intrinsic vulnerability. They combined it with a high-resolution land use/land cover map to evaluate the groundwater vulnerability.

The article will present a methodology for constructing a multidisciplinary composite index for assessing the groundwater

vulnerability to contamination in JTLATS in light of the water conflict and climate change. This study is the first in which multidisciplinary composite indicators are used in assessing the vulnerability of transboundary aquifers, using remote sensing data and large databases. In addition to the development that has been made in the way of weighing the individual components of the composite index through the use of the correspondence analysis method. The study of vulnerability through different periods also shows the impact of environmental, political, and social conditions on changing the vulnerability of the transboundary aquifer.

Materials and methods

Study area

The JTLTAS is situated beneath a plateau area, stretching from northern Syria into south-eastern Anatolia in Turkey. It extends across the Upper Jezira Basin, in the space between Qamishli, Hasakah, Aleppo, Raqqah in Syria, and Sanliurfa and Kiziltepe in Turkey. It also extends to Tal Afar and the Ba'aj district in Iraq, as shown in Fig (1). The total population of the aquifer area is approximately 15,251 million. The southern part of the Jezira Tertiary Limestone Aquifer System lies in a semiarid climatic zone, while the northern mountainous region reaches into more humid climatic zones. The JTLATS is exposed on the surface in the highlands in the northern part of the catchment. Volcanic rocks cover the aquifer in the Karaca Dag Mountain area and by Miocene to Quaternary sedimentary deposits in the plains to the south. The JTLATS consists of three formations in Ras al-Ain area: two karstic formations that constitute the main aquifers and a massive formation in the middle that is water-bearing, mainly in tectonically active faulted zones (ACSAD et al., 2003). According to Kattan (2018), Stadler et al. (2012), and Avci et al. (2018), a section of JTLATS consists of alluvial formations mainly along the Euphrates River and in other parts of the aquifer in both Syria and Turkey.

Average Annual Precipitation varies from around 300 mm in the south to 800 mm at the top of the Karaca Dag Mountains (Burdon and Safadi, 1963). Precipitation is concentrated during the cool winter season (0°C-10°C). No rain falls during summer when temperatures rise between 30ºC and 45ºC. Mean annual potential evaporation is 1,000-1,300 mm (Kattan, 2002). The top of the aquifer system descends from more than 1,000 m in the outcrop areas in the highlands to 200-400 m in the border area between Syria and Turkey (UN-ESCWA. 2013).

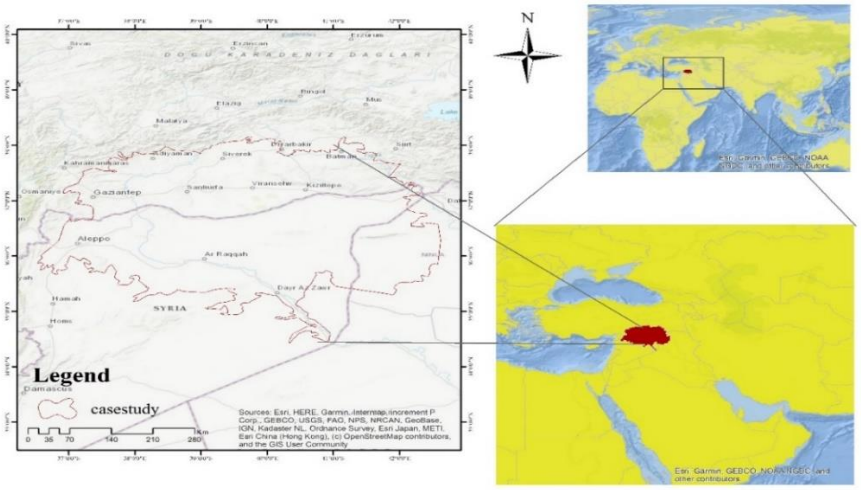

Fig. 1- Jezira Tertiary Limestone Transboundary Aquifer System

 DOI: 10.22055/JISE.2022.40701.2027

Groundwater vulnerability index development

This section detail the steps involved in developing a groundwater vulnerability index (GVI), from selecting individual components to weight, aggregation, and the final index. The methodology section Fig (2) will also clarify and justify each stage of index development.

The distributed index was developed using an overlay and index method and implemented in the ArcGIS to show the Spatio-temporal distribution of groundwater vulnerability.

Theoretical framework and individual components selection

The presence of groundwater, its availability, or even the sustainability of its extraction does not necessarily mean its usability, especially in arid and semiarid areas such as JTLTAS. Therefore, we will assess the groundwater vulnerability to contamination using a multi-pronged index that considers the study area's hydrogeological, socioeconomic, and political conditions. The first step in constructing a composite index is to provide a conceptual basis for selecting the components influencing the multidimensional phenomenon to be evaluated. The index will integrate two types of groundwater vulnerability to contamination, the intrinsic and the specific vulnerability. Given that part of the aquifer is alluvial Fig (3b), we will assume the possibility of applying the DRASTIC model to study the intrinsic vulnerability. The specific vulnerability will be studied through the impact of land use, population density, and governance indicators. It can theoretically divide the individual components into two parts, the static and dynamic components, so it is possible to monitor the temporal changes of the groundwater vulnerability index during the study periods. The greater the index values, the greater the possibility of the presence of contamination in the aquifer, and it will be studied during three different periods as follows:

- The first period is (2003-2007), characterized by economic growth, expansion of self-sufficiency policies in Syria and Turkey, and political instability in Iraq.
- The second period is (2007-2011), characterized by the spread of drought in the region (Mohtadi, 2013; Worth, 2010), coinciding with the global economic crisis.
- The third period is (2011-2017), characterized by political instability in Syria and Iraq.

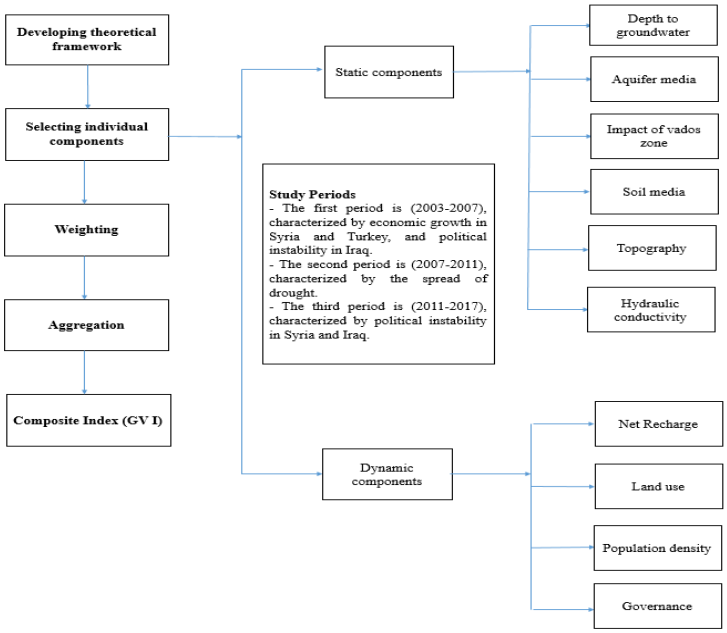

Fig. 2- Flowchart of the proposed methodology

Table 1- Distribution of eigenvalues and cumulative % of system variance

Vector	Study Period (2003-2007)					Study Period (2007-2011)					Study Period (2011-2017)				
	V1	V2	V3	V4	V5	V1	V2	V3	V4	V5	V1	V2	V3	V4	V5
Eigenvalue	0.07	0.053	0.041	0.029	0.015	0.07	0.056	0.042	0.033	0.013	0.071	0.054	0.041	0.032	0.013
Cum.Var %	31.24	54.74	73.01	85.67	92.43	31.00	55.75	74.28	88.93	94.59	31.64	55.97	74.32	88.67	94.47

Table 2- The results of CA variable loading values and adjusted variable weight

Variable	Variable Loading and Adjusted Weight in Study Period (2003-2007)						Variable Loading and Adjusted Weight in Study Period (2007-2011)						Variable Loading and Adjusted Weight in Study Period (2011-2017)					
	V1	V2	V3	V4	V5	Adjusted Weight	V1	V2	V3	V4	V5	Adjusted Weight	V1	V2	V3	V4	V5	Adjusted Weight
Depth to Water	0.01	0.0001	0.1	0.02	0.29	2.33	0.1	0.001	0.14	0.02	0.77	4.62	0.01	0.0003	0.15	0.01	0.77	4.58
Recharge	0.18	0.04	0.03	0.001	0.64	3.94	0.03	0.03	0.002	0.03	0.15	1.7	0.16	0.003	0.0002	0.003	0.19	1.88
Aquifer Type	0.074	0.0007	0.57	0.015	0.003	3.62	0.1	0.0009	0.55	0.04	0.12	3.59	0.08	0.001	0.62	0.001	0.12	3.88
Soil Media	0.088	0.27	0.36	0.008	0.002	2.66	0.14	0.26	0.30	0.004	0.07	2.41	0.1	0.27	0.28	0.05	0.04	2.3
Topography	0.25	0.34	0.41	0.002	0.006	2.88	0.26	0.25	0.49	0.001	0.0002	3.31	0.24	0.30	0.45	0.01	0.0001	3.09
Impact of Vados Zone	0.07	0.0007	0.57	0.01	0.003	3.62	0.1	0.001	0.55	0.04	0.12	3.59	0.08	0.001	0.62	0.001	0.1	3.88
Hydraulic Conductivity	0.87	0.07	0.04	0.004	0.007	5	0.85	0.1	0.02	0.01	0.0001	5	0.86	0.06	0.04	0.006	0.001	5
Land Use	0.001	0.57	0.26	0.16	0.0005	3.62	0.04	0.59	0.19	0.17	0.0001	3.78	0.01	0.60	0.10	0.27	0.001	3.79
Population Density	0.01	0.26	0.04	0.67	0.003	4.08	0.01	0.29	0.02	0.67	0.002	4.15	0.025	0.29	0.13	0.55	0.001	3.56
Governance	0.31	0.02	0.18	0.004	0.001	2.43	0.33	0.05	0.27	0.01	0.07	2.55	0.34	0.05	0.22	0.003	0.08	2.58

The data came in different spatial resolutions. We resampled the data layers to fit the proposed resolution of the GIS model. We proposed a resolution of 0.22 km × 0.22 km for this study. We consider this decision a reasonable compromise between different choices for different data sets, computing limitations, and regional extent.

Static individual components (DASTIC)

The individual static components were selected based on the DRASTIC model used to assess the groundwater vulnerability (Aller et al., 1987).

Depth to groundwater

The groundwater depth is a critical factor because it determines the depth of the aquifer material through which the pollutant must move to reach the aquifer (Rahman, 2008). Depth to groundwater is considered a dynamic factor, but due to the lack of reliable data in the JTLATS, it was assumed to be a static factor during the study. Depth data for groundwater were determined using a global water table pattern map developed by Fan et al. (2013) in 1 x 1 km grid cells. According to Aller et al. (1987), the value of D was rated as shown in Table (A1) in the supplemental online data and Fig (3a).

Aquifer Media (A)

Aquifer media refers to the type of consolidated or unconsolidated material drains the aquifer. The groundwater vulnerability increases if the size of the grains or fractures through the aquifer increases (Yahia and Bouabid, 2011). Aquifer-forming media was extracted from the high-resolution global lithological database (GliM) of Hartmann and Moosdorf (2012) and the global permeability estimates of Gleeson et al. (2014). Categories related to aquifer media, with their rate according to Aller et al. (1987), are shown in Table (A2) in the supplemental online data and Fig (3b).

Impact of vadose zone (I)

The vadose zone is the unsaturated zone above the groundwater level and below the soil layer, affecting the contaminant's stay in the unsaturated zone. Similar to parameter A, the method used to determine the vadose zone material is based on GLiM data. The parameter ratings are shown in Table (A2) in the supplemental online data and Fig (3c).

Soil media (S)

S refers to the upper layer of the vadose zone where biological activity occurs. (S) has a significant impact on groundwater recharge. The soil also controls the attenuation of pollutants through biodegradation, filtration, volatilization, absorption, and adsorption (Aller et al., 1987). The soil map of JTLATS was inferred from the data processed by Hengl et al. (2018), and the rating is shown in Table (A1) in the supplemental online data and (Fig. 3d).

Topography (T)

The topography indicates the slope variation in the models based on DRASTIC; slope governs the probability that the pollutant is available on the Earth's surface for a sufficient period to infiltrate. For this study, the slope map (%) of JTLATS was inferred from the data processed by Hengl et al. (2018), and the rating is shown in Table (A1) in the supplemental online data and (Fig. 3e).

Hydraulic conductivity (C)

Hydraulic conductivity is a measure of an aquifer's ability to transport water. It determines the velocity of pollutant transmission and thus residence time and attenuation potential (Rahman, 2008). The hydraulic conductivity map was obtained from the global hydrogeological map of permeability and porosity presented by Gleason et al. (2014).

The global permeability map is presented in log permeability (log (k)). We converted the permeability k into the hydraulic conductivity K as follows:

$$K = \frac{k * rho * g}{mu} \quad (1)$$

Where K (m/s) is hydraulic conductivity, rho (kg/m^3) is the fluid density, g (m/s^2) is the gravity acceleration = 9.8 m/s^2 and mu (kg/m.s or Pa.s) is the fluid viscosity. The rating of hydraulic conductivity (m/day) is shown in Table (A1) and Fig (3f).

Dynamic individual components

We have four dynamic parameters that change during the study periods: net recharge, land use, population density, and governance.

Net Recharge (R)

Net recharge is the amount of surface water seeping into the ground and reaching groundwater level. It is an effective means of transporting pollutants to groundwater during leaching. Many studies have suggested that climate change will directly affect groundwater recharge (Gogu et al., 2000; Raupach et al., 2013). Given the droughts that were subjected to the study area (Mohtadi, 2013; Worth, 2010) and the absence of dynamic data for the recharge process at the level of the study area, the relationship shown in Equation (1) was used to infer the trends of groundwater recharge in response to climate change during the three study periods.

$$R = P - ET - Q \quad (2)$$

Here R is the recharge (mm), P is the total precipitation (mm), ET is evapotranspiration (mm), and Q is the runoff in mm. Data will be extracted from GLDAS Noah Land Surface Model L4 monthly 0.25 x 0.25 degree V2.1. According to Aller et al. (1987), the R-value was rated as shown in Table (A1) and Fig (4a).

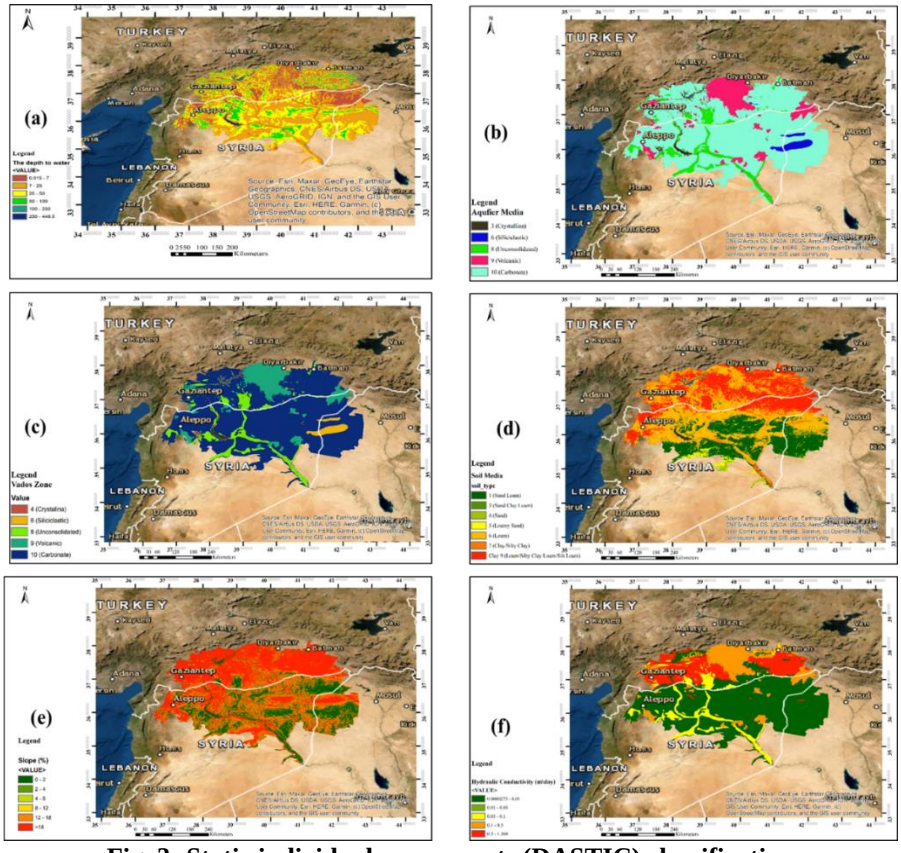

Fig. 3- Static individual components (DASTIC) classification

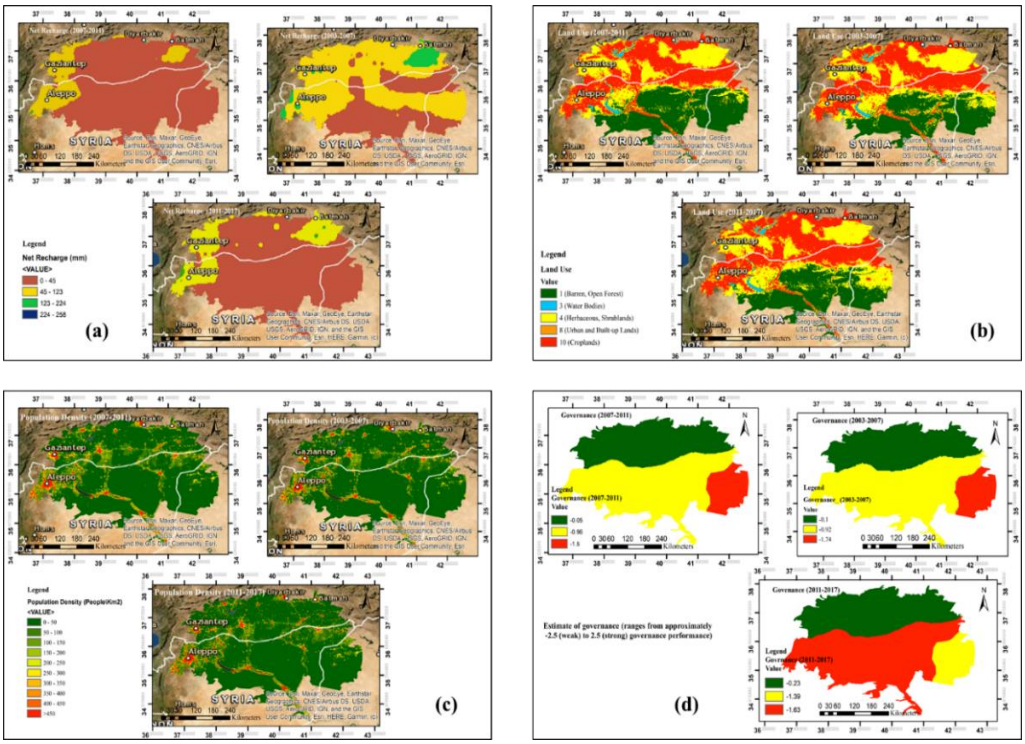

Fig. 4- Dynamic individual components classification

Land use (L)

Land use has a direct link to groundwater contamination. Pollutants generated by human activities on the land surface seep into the Earth and contaminate groundwater resources (Lutz et al., 2011). Concerning the study area being the main food reservoir for both Syria and Turkey, the spread of agricultural lands in the region is significant, especially with the efforts made by the governments to increase the irrigated area (Al-Ansari et al., 2018). The spread of agricultural lands results in fertilizers, which are a significant source of groundwater pollution. The land use map was obtained from MODIS Land Cover Type Product (MCD12Q1) (Friedl and Menashe 2019). The land-use factor was rated as follows in Table (3) in the supplemental online data and (Fig. 4b).

Population density (P)

The population density is usually represented as the number of people per square kilometer (people/km^2). Indeed, a recent study by Lapworth et al. (2017) showed that fecal waste is the primary source of pollution in urban (and rural) groundwater, mainly with high-density housing with poor and inadequate sanitation facilities and treatment of fecal waste.

Population density map was obtained from World Bank Database at a resolution of 1 Km and rated according to Ouedraogo et al. (2020), as shown in Table (A3) in the supplemental online data and Fig (4c).

Governance (G)

Governance is one of the most critical factors affecting the sustainability of water resources in general and groundwater in particular (Ostrom, 1990). The World Bank has defined six factors to assess the governance index in countries. These factors are voice and accountability, government effectiveness, regulatory quality, the rule of law, corruption control, political stability, and absence of violence/terrorism. The study area is considered one of the sensitive areas for governance factors concerning groundwater, especially considering the circumstances that have passed over the region.

Annual country-level governance datasets between 2003 and 2017 were obtained from the World Bank's open access webpage. The six governance dimensions were then arithmetically averaged to produce the overall governance data, which was then rasterized (0.002-degree) to allow for spatial aggregation with the other components composing the vulnerability index (Fig. 4d). The governance index was evaluated by the World Bank between +2.5 as an indicator of the strength to -2.5 as an indication of weak governance. After calculating the index for each country, we rerated the governance values from 10.

Weighting

Determining the relative importance of index components requires explicit weighting during the aggregation process. From the statistical perspective, variable weights are meaningful only if the variables are independent. It is not the case in our study. For example, recharge is highly related to terrain, where the recharge capacity is high in flat areas and minor in steep areas. If variables are correlated, creating a statistically significant composite index is still possible, provided the associated correlations are identified and neutralized.

In these cases, the most appropriate techniques to adopt are eigenvector methods (Pacheco and Landim, 2005). Therefore, we will rely on eigenvector techniques. These algorithms transform the original correlated features into a new set of uncorrelated variables (vectors). A large portion of the data variance is concentrated on a few of them (Pacheco and Fernandes, 2013). Several eigenvector techniques are available: factor analysis, principal component analysis, correspondence analysis, etc. If the input data are categorized as qualitative-categorical data, the preferred approach is correspondence analysis (CA), so we used it in our study.

Correspondence analysis converts N correlated variables into k uncorrelated common vectors. The correspondence analysis mechanism can be found in Heiser and Meulman (1983), Heijden et al. (1989) and Pacheco and Fernandes (2013). Briefly, the transformation of variables into vectors is described as follows:

$$V_i = \sum_{j=1}^{N} v_{ij} X_j \;\; ; \;\; 1 \le i \le k \qquad (3)$$

Where X_j is one of the p variables (ten variables in our study), Vi is one of the k (< p) uncorrelated common vectors (the primary trend of data variation), and v_{ij} is the contribution of variable j to the common vector i, usually called loading.

Aggregation

After assigning weights to each component, the component scores required aggregation into a composite score. There are two main aggregation methods: linear additive aggregation and non-linear multiplicative aggregation. The properties of these two methods are fundamentally different (Choo and Wedley, 2008). The linear additive method used in the composite index's theoretical framework allows full compensation. However, non-linear multiplier aggregation allows partial or less substitution (Joint Research Centre-European Commission, 2008). This paper assumes that linear additive aggregation Equation (4) is best suited for the groundwater vulnerability index, taking full compensability within different dimensions (e.g., good levels of governance can compensate for higher vulnerabilities of groundwater caused by land use).

$$\begin{aligned}(GVI)_i = {} & (D_{i,r} \times D_{i,w}) + (R_{i,r} \times R_{i,w}) + (A_{i,r} \times A_{i,w}) \\ & + (S_{i,r} \times S_{i,w}) + (T_{i,r} \times T_{i,w}) \\ & + (I_{i,r} \times I_{i,w}) + (C_{i,r} \times C_{i,w}) \\ & + (L_{i,r} \times L_{i,w}) + (P_{i,r} \times P_{i,w}) \\ & + (G_{i,r} \times G_{i,w})\end{aligned} \qquad (4)$$

Where:

GVI_i is Groundwater Vulnerability Index in the period i. As previously defined, D, R, A, S, T, I, C, L, P, G are the index components, and the subscripts r, i, and w are the corresponding rating for period i and weights.

 DOI: 10.22055/JISE.2022.40701.2027

Table 3- GVI results

	Index	Max value	Min value	Mean value	Area with very high vulnerability (%)		Area with high vulnerability (%)		Area with moderate vulnerability (%)		Area with low vulnerability (%)		Area with very low vulnerability (%)	
					Country	Aquifer	Country	Aquifer	Country	Aquifer	Country	Aquifer	Country	Aquifer
Syria	2003-2007	283.37	93.35	175.46	0.1	0.05	7.92	4.00	46.8	23.60	44.98	22.64	0.2	0.14
	2007-2011	304.44	100.22	181.58	0.1	0.05	11.7	5.9	39.2	19.73	48.81	24.57	0.19	0.1
	2011-2017	304.24	104.32	187.68	0.2	0.1	15.31	7.71	45.33	22.82	39.04	19.65	0.1	0.05
Iraq	2003-2007	240.75	100.49	158.21	-	-	0.42	0.04	21.64	2.42	72.97	7.91	4.99	0.54
	2007-2011	269.55	97.89	171.24	0.03	0.003	3.76	0.41	37.78	4.1	56.54	6.13	2.12	0.23
	2011-2017	266.82	107.37	178.96	0.04	0.004	5.08	0.55	47.1	5.11	46.77	5.07	1.24	0.13
Turkey	2003-2007	293.76	87.61	195.97	0.43	0.14	19.12	6.41	69.32	23.22	10.96	3.71	0.22	0.15
	2007-2011	308.03	87.68	204.75	0.48	0.16	21.25	7.11	68.56	22.93	9.56	3.23	0.18	0.06
	2011-2017	303.1	88.96	209.56	0.68	0.23	36.8	12.31	56.33	18.84	6.16	2.1	0.15	0.05

Results and discussion

Ratings of GVI variables

Ratings of each parameter are illustrated in Tables (A1, A2 and A3), which vary from 1 to 10, with higher values describing greater vulnerability to contamination.

The D map is represented in Figure (3a). The depth to groundwater rate ranges from 0 to 449.5 m across the JTLATS. The heights are shallow in the north-eastern Syria region and along the Euphrates river's tributaries. Shallow depths also characterize the volcanic rock region that extends through the provinces of Diyarbakir and Urfa.

The A map is shown in Figure (3b). Carbonate rocks (mainly limestone) are the leading aquifer media, and a rate of 10 has been assigned to these rocks. The unconsolidated rocks spread along the Euphrates river, and a rate of 8 was given to them.

The soil texture S map is represented in Fig. (3d). Sandy loam soil is spread in the southern part of the aquifer, while the loam soil is located in the central region, on both sides of the Euphrates river and its tributaries. Figure 3e shows the T map representing the slope. High slopes dominate the northern section of the aquifer (the Turkish area. In comparison, the slopes are gentle in the southern part of the aquifer.

The I map is shown in Figure (3c). The same data and method were used to determine I and A.

Figure (3f) shows the hydraulic conductivity map. Hydraulic conductivity values were rated into five categories. The low hydraulic conductivity values (<0.01 m/day) dominate the central and southern sections of the aquifer (the Syrian and Iraqi units). In contrast, the conductivity values are greater (0.03-0.1 m/day) around the Euphrates river. High hydraulic conductivity values dominate in the northern part of the aquifer (> 0.3 m/day).

Figure (4a) shows the recharge map R. A clear difference was observed in the recharge rates during the three study periods. For example, in the period (2003-2007), the low recharge rates (0-45 mm) were concentrated in 36.8% of the aquifer area in the south and the east at the border triangle between Syria, Iraq, and Turkey. This percentage reached 86.6% in the second period (2007-2011).

The land use map is represented in Figure (4b). Land use was divided into six categories and rated as shown in Table (A3). The land use map changed during the three study periods in Syria, Iraq, and Turkey. It is noticed from Figure 4b that the ratio of the extent of croplands decreased, and the bare lands increased in Syria in the period (2007-2011), which was characterized by drought waves. In comparison, the area of croplands in Turkey increased during the study periods and was not affected by drought.

Figure (4c) shows the population density map. The population density was divided into ten categories. It is noticed that the population density is increasing in the main cities (Aleppo, Gaziantep, Diyarbakir) and its suburbs, in addition to areas near the Euphrates River and its tributaries.

The governance map is represented in Figure (4d). The values of the governance parameter were rerated between 1 as an indicator of strong governance and lower groundwater vulnerability and 10 as an indicator of weak governance and greater groundwater vulnerability. It is observed from Figure 4d a change in the values of governance, especially for Syria, in the period between 2011-2017, when Syria witnessed a political crisis and the spread of terrorism.

The weighting of GVI variables

After rating the variables as previously explained, a weighing process was conducted for the components using the correspondence analysis technique after selecting 100 random spatial samples distributed over the entire aquifer area for each of the ten components. The CA was computed using R (R Core Team, 2019), an open-access software. Application of Correspondence Analysis to data resulted in the identification of five common vectors, V1, V2, V3, V4, and V5, which in total explain 92.43% of system variance in the first period (2003-2007), 94.59% in the second period (2007-2011), and 94.47% in the third period (2011-2017). Table (1) shows the distribution

of eigenvalues and cumulative percentage of the system variance for the vectors.

Each vector load was rescaled to values (1-5) using the harmonization formula provided by Pacheco and Fernandes (2013), as seen in Equation (5). These new sets of weights were called adjusted variable weights. The contributions of variables to common vectors and adjusted variables' weight during the study periods are depicted in Table (2).

$$w_{adj} = \frac{w_{j,max} \times v_{j,max} - (w_{j,max} - w_{j,min}) \times (v_{j,max} - v_j)}{v_{j,max}} \quad (5)$$

Where max and min represent the maxima and minima of variable weights (w_j) and loadings (v_j).

It is evident in the three periods that the hydraulic conductivity component C is the explicative variable for the V1 vector, which explains about 31% of the total variance of the system. It also notes that the land-use L is an explicative variable for vector V2, which explains about 23% of the total variance. I, S, T, and A are explicative variables for the vector V3, which explains about 19% of the system's variance. In addition, P is the explicative variable for vector V4, which explains about 12% of the system's variance. As for the vector V5, it is noted that in the stage (2003-2007), recharge R was the explicative variable and, to a lesser degree, the depth to groundwater. In the second time stage (2007-2011), which was characterized by the spread of drought up to the third time stage (2011-2017), which was characterized by political instability, the depth to groundwater became the explicative variable for vector V5 at the expense of groundwater recharge.

Aggregation and aquifer vulnerability

Depending on the ratings of the components (Tables 1, 2 and 3) and the weights calculated for each component and across the three study periods Table (2), the values of the groundwater vulnerability index were calculated according to the linear additive aggregation system as shown in Equation (4). Figure (5) shows the distribution of vulnerability in the JTLATS during the study periods.

We categorized the JTLATS into five zones corresponding to very low, low, moderate, high, and very high vulnerability. Figure (5) shows a low vulnerability in the southern regions of the aquifer, as these regions are mainly characterized as bare regions with no human activity. In comparison, the areas with high vulnerability are primarily spread in the northern and western parts of the JTLATS and along the Euphrates river, where human activities are active. It is noted from Table (3) that about 7.9% of the area of the Syrian section of the aquifer was highly vulnerable in the first study period (2003-2007), while this percentage rose to 11.7% and 15.3% in the second and third periods respectively. In Turkey, regions with high vulnerability increased from 19% in the first period to 21% and 36.8% in the second and third periods, respectively. In Iraq, 72.9% of the area in the first period was of low vulnerability. This percentage decreased in the second and third periods, and the area of regions with medium vulnerability increased.

Table (3) also shows the min, max, and mean index values in Syria, Iraq, and Turkey, in addition to the percentage distribution of the area region with very high, high, medium, low, and very low vulnerabilities concerning the area of each country in the aquifer and relation to the area of the aquifer as a whole.

The results of this study are consistent with the findings of Yesilnacar and Gulluoglu (2008) about the impact of the operation of the GAP project on the quality of groundwater in the Harran Plain, where it indicated that most of the groundwater samples exceeded the standard limits of nitrate concentration affected by surface irrigation. The study's results are also consistent with what Kattan (2018) found about the increase in groundwater salinity on the Euphrates River bed in Syria.

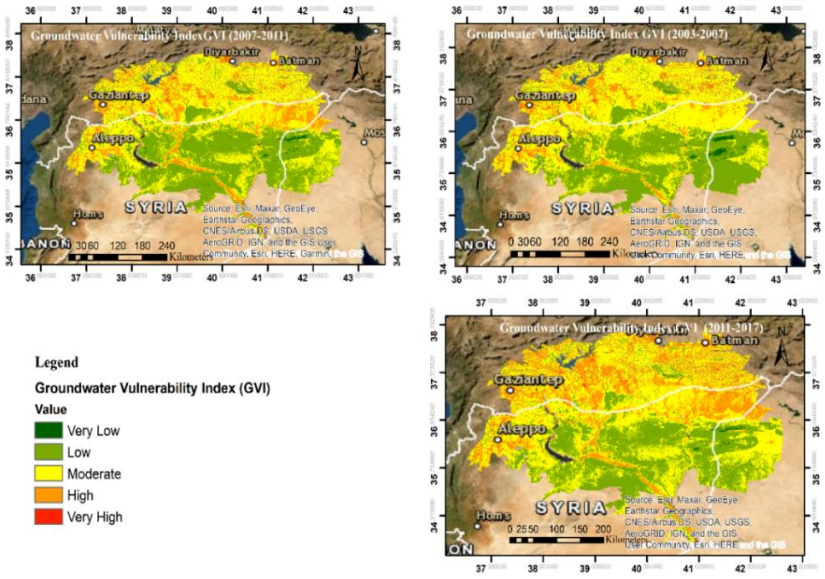

Fig. 5- Distribution of vulnerability in the JTLATS

It is worth noting that the groundwater flow direction, in this case, has a transboundary effect on the management process of the aquifer. According to ESCWA and B. G. R. (2013), the groundwater flow direction in the aquifer is from Turkey to Syria and Syria to Iraq. Consequently, governments and policymakers must realize that the impacts on aquifers will affect their neighbors. Ensuring good water quality, sustainable extraction rates, and adapting development plans, considering the principle of not harming others, will help prevent negative impacts on riparian countries.

Conclusion

Based on remote sensing data and large databases, a multidisciplinary composite index has been built to assess the groundwater vulnerability in the JTLATS. The study period was divided into three periods, each with different climatic, political, and social conditions. The first period 2003-2007, where this stage was characterized by economic growth in Syria and Turkey, while political instability prevailed in Iraq. The second phase, 2007-2011, is characterized by successive droughts that hit the region and the food and global economic crisis. The third stage is 2011-2017, characterized by political instability in Syria and Iraq. After selecting the index's components and rating them based on the assumptions of the DRASTIC model and other researchs, the correspondence analysis method was chosen to weigh the individual components. The additive linear aggregation was also used to build the groundwater vulnerability index, assuming that this method allows full compensation for weak performance in one aspect with a strong performance in other aspects. The JTLATS was categorized into five zones: very low, low, moderate, high, and very high vulnerability. The results showed a low vulnerability in the southern regions of the aquifer, as these regions are mainly bare regions with no human activity. In comparison, the areas with high vulnerability are primarily spread in the northern and western part of the JTLATS and along the Euphrates river, where human activities in general and agricultural activities, in particular, are active. The change in the index values for the three countries can be attributed to the conditions that governed each

study period, distinguished as dynamic parameters. Drought and the change in the governance indicator can explain the difference in the index values in Syria and Iraq. While it seems that Turkey's plans to increase the irrigated areas were not much affected by the drought that hit the region, where the increase in the areas planted with crops during the study periods in Turkey can have the most significant effect in increasing the scope of areas with high and medium vulnerability. Given the scarcity of water in both Syria and Iraq, the long history of conflict over water resources in the study area between the riparian countries, and the importance of groundwater as a strategic source for securing the various human needs of individuals and the plans of governments in development, the importance of regional studies appears as an effective tool for joint management.

Author contributions

All authors conceived and designed the study. Mohamed Al-Mohamed collected the data, performed the analysis, and wrote the paper. All authors read and approved the final manuscript.

Funding sources

This research did not receive any specific grant from public, commercial, or not-for-profit funding agencies.

References

1- ACSAD, GDTKB and GCHS (Arab Center for the Studies of Arid Zones and Dry Lands, 2003. General Directorate for Tigris and Khabour Basins; General Corporation for Hydrological Studies. Project of Preparation of a Database and a Mathematical Model for the Northern Part of the Khabour Basin. In The Mathematical Model (General Report). Damascus.

2- Al-Ansari N, Adamo N, Knutsson S, Laue J, 2018. Geopolitics of the Tigris and Euphrates basins. *Journal of Earth Sciences and Geotechnical Engineering*, *8*(3), 187-222.

3- Allan T, 2012. *The Middle East water question: Hydropolitics and the global economy*. Bloomsbury Publishing.

4- Aller L, Bennett T, Lehr J, Petty R J, Hackett G, 1987. DRASTIC: A standardized system for evaluating ground water pollution potential using hydrogeologic settings. US Environmental Protection Agency. *Washington, DC, 455*.

5- Avci H, Dokuz U E, Avci A S, 2018. Hydrochemistry and groundwater quality in a semiarid calcareous area: an evaluation of major ion chemistry using a stoichiometric approach. Environmental monitoring and assessment, 190(11), 1-16.

6- Barbulescu A, 2020. Assessing groundwater vulnerability: DRASTIC and DRASTIC-like methods: a review. *Water*, *12*(5), 1356.

7- Burdon, D.J. and Safadi, C., 1963. Ras-el-ain: The great karst spring of mesopotamia: An hydrogeological study. *Journal of Hydrology*, *1*(1), pp.58-95.

8- Chao N, Luo Z, Wang Z, Jin T, 2018. Retrieving groundwater depletion and drought in the Tigris-Euphrates Basin between 2003 and 2015. *Groundwater*, *56*(5), 770-782.

9- Choo E U, Wedley W C, 2008. Comparing fundamentals of additive and multiplicative aggregation in ratio scale multi-criteria decision making. *The Open Operational Research Journal*, *2*(1).

10- Fan, Y., Li, H., & Miguez-Macho, G. (2013). Global patterns of groundwater table depth. Science, 339(6122), 940-943.

11- Fraser C M, Kalin R M, Kanjaye M, Uka Z, 2020. A methodology to identify vulnerable transboundary aquifer hotspots for multi-scale groundwater management. *Water International*, *45*(7-8), 865-883. https://doi.org/10.1080/02508060.2020.1832747.

12- Friedl, M., & MCD12Q1, S. M. D. v006. MODIS. Terra+ Aqua land cover type yearly L3 global, 500.. https://doi.org/10.5067/MODIS/MCD12Q1.006.

13- Ghadimi M, Zangenehtabar S, Malekian A, Kiani M, 2022. Groundwater vulnerability assessment in a karst aquifer: a case study of western Iran. *International Journal of Environmental Science and Technology*, 1-14.

14- Gogu, R. C., & Dassargues, A. (2000). Current trends and future challenges in groundwater vulnerability assessment using overlay and index methods. *Environmental geology*, *39*(6), 549-559.

15- Gleeson T, Smith L, Moosdorf N, Hartmann J, Dürr H H, Manning A H, Jellinek A M, 2011. Mapping permeability over the surface of the Earth. *Geophysical Research Letters*, *38*(2). http://dx.doi.org/10.1029/2010GL045565.

16- Gleeson T, Moosdorf N, Hartmann J, Van Beek L P H, 2014. A glimpse beneath Earth's surface: GLobal HYdrogeology MaPS (GLHYMPS) of permeability and porosity. *Geophysical Research Letters*, *41*(11), 3891-3898.

17- Hartmann J, Moosdorf N, 2012. The new global lithological map database GLiM: A representation of rock properties at the Earth surface. *Geochemistry, Geophysics, Geosystems*, *13*(12). http://dx.doi.org/10.29/2012GC004370.

18- Heijden P V D, Falguerolles A, Leeuw J, 1989. A combined approach to contingency table analysis using correspondence analysis and log-linear analysis. *Applied Statistics*, *38*(2), 249-292. https://doi.org/10.2307/2348058.

19- Heiser W J, Meulman J, 1983. Analyzing rectangular tables by joint and constrained multidimensional scaling. *Journal of Econometrics*, *22*(1-2), 139-167. https://doi.org/10.1016/0304-4076(83)90097-0

20- Hengl T, 2018. Soil texture classes (USDA system) for 6 soil depths (0, 10, 30, 60, 100 and 200 cm) at 250 m (v0.2) [Data set]. Zenodo. https://doi.org/10.5281/zenodo.2525817.

21- Hengl T, 2018. Global DEM derivatives at 250 m, 1 km and 2 km based on the MERIT DEM (1.0) [Data set]. Zenodo. https://doi.org/10.5281/zenodo.1447210

22- Huan H, Zhang B T, Kong H, Li M, Wang W, Xi B, Wang G, 2018. Comprehensive assessment of groundwater pollution risk based on HVF model: a case study in Jilin City of northeast China. *Science of the total Environment*, *628*, 1518-1530. https://doi.org/10.1016/j.scitotenv.2018.02.130.

23- IGRAC U. I, 2015. Transboundary aquifers of the world [map]. 15 Scale 1: 50 000 000.

24- Joint Research Centre-European Commission, 2008. *Handbook on constructing composite indicators: methodology and user guide*. OECD publishing.

25- Kattan, Z., 2018. Using hydrochemistry and environmental isotopes in the assessment of groundwater quality in the Euphrates alluvial aquifer, Syria. *Environmental earth sciences*, *77*(2), pp.1-18.

26- Kattan Z, 2002. Effects of sulphate reduction and geogenic CO_2 incorporation on the determination of ^{14}C groundwater ages–a case study of the Palaeogene groundwater system in north-eastern Syria. *Hydrogeology journal*. https://doi.org/10.1007/s10040-002-0199-3.

27- Lapworth D J, Nkhuwa D C W, Okotto-Okotto J, Pedley S, Stuart M E, Tijani M N, Wright J J H J, 2017. Urban groundwater quality in sub-Saharan Africa: current status and implications for water security and public health. *Hydrogeology Journal*, *25*(4), 1093-1116. https://doi.org/10.1007/s10040-016-1516-6.

28- Lezzaik K, Milewski A, Mullen, J, 2018. The groundwater risk index: Development and application in the Middle East and North Africa region. *Science of the Total Environment*, *628*, 1149-1164. https://doi.org/10.1016/j.scitotenv.2018.02.066.

29- Lutz A, Thomas J M, Keita M, 2011. Effects of population growth and climate variability on sustainable groundwater in Mali, West Africa. *Sustainability*, *3*(1), 21-34. https://doi.org/10.3390/su3010021.

30- McCracken M, 2017. *Measuring transboundary water cooperation: options for Sustainable Development Goal Target 6.5* (pp. 1-88). Stockholm, Sweden: Global Water Partnership (GWP).

31- Mohtadi S, 2013. Climate change and the Syrian uprising. *Bulletin of the Atomic Scientists*, *16*.

32- Ouedraogo I, Defourny P, Vanclooster M, 2016. Mapping the groundwater vulnerability for pollution at the pan African scale. *Science of the Total Environment*, *544*, 939-953. https://doi.org/10.1016/j.

33- Ouedraogo I, Girard A, Vanclooster, M, Jonard F, 2020. Modelling the temporal dynamics of groundwater pollution risks at the african scale. *Water*, *12*(5), 1406. https://doi.org/10.3390/w12051406.

34- Ostrom E, 1990. *Governing the commons: The evolution of institutions for collective action*. Cambridge university press.

35- Pacheco F A, Fernandes L F S, 2013. The multivariate statistical structure of DRASTIC model. *Journal of Hydrology*, *476*, 442-459. https://doi.org/10.1016/j.jhydrol.2012.11.020.

36- Pacheco F A L, Landim P M B, 2005. Two-way regionalized classification of multivariate datasets and its application to the assessment of hydrodynamic dispersion. *Mathematical geology*, *37*(4), 393-417. https://doi.org/10.1007/s11004-005-5955-1.

37- Stadler S, Geyh M A, Ploethner D, Koeniger P, 2012. The deep Cretaceous aquifer in the Aleppo and Steppe basins of Syria: assessment of the meteoric origin and geographic source of the groundwater. Hydrogeology Journal, 20(6), 1007-1026.

38- Team R. C, 2019. R: A language and environment for statistical computing. Vienna, Austria.

39- Rahman A, 2008. A GIS based DRASTIC model for assessing groundwater vulnerability in shallow aquifer in Aligarh, India. *Applied geography*, *28*(1), 32-53. https://doi.org/10.1016/j.apgeog.2007.07.008.

40- Rivera A, Candela L, 2018. Fifteen-year experiences of the internationally shared aquifer resources management initiative (ISARM) of UNESCO at the global scale. *Journal of Hydrology: Regional Studies*, *20*, 5-14. https://doi.org/10.1016/j.ejrh.2017.12.003.

41- Raupach M R, Haverd V, Briggs P R, 2013. Sensitivities of the Australian terrestrial water and carbon balances to climate change and variability. *Agricultural and Forest Meteorology*, *182*, 277-291. https://doi.org/10.1016/j.agrformet.2013.06.017.

42- Taghavi N, Niven R K, Paull D J, Kramer M, 2022. Groundwater vulnerability assessment: A review including new statistical and hybrid methods. *Science of The Total Environment*, 153486.

43- UN-ESCWA, B.G.R., 2013. Inventory of shared water resources in Western Asia: Chapter 6 Jordan River Basin. United Nations Economic and Social Commission for Western Asia. *Federal Institute for Geosciences and Natural Resources, Beirut*.

44- World Bank. World Development Indicators database, edited, Washington DC, USA.

45- Worth R F, 2010. Earth is parched where Syrian farms thrived. *New York Times*, *13*.

46- Yahia A, Bouabid El M, 2011. Assessment of aquifer vulnerability based on GIS and ARCGIS methods: a case study of the Sana'a Basin (Yemen). *Journal of Water Resource and Protection*, *2011*.

47- Yesilnacar M I, Gulluoglu M S, 2008. Hydrochemical characteristics and the effects of irrigation on groundwater quality in Harran Plain, GAP Project, Turkey. *Environmental Geology*, *54*(1), 183-196. https://doi.org/ 10.1007/s00254-007-0804-9.

Appendix

Table A1- Rating of the DRASTIC parameters (Aller et al., 1987).

Depth to groundwater		Net recharge		Soil media		Topography %		Hydraulic conductivity	
Interval	Rating	Interval	Rating	Interval	Rating	Interval	Rating	Interval	Rating
0-7	10	0-45	1	Sand loam	1	0-2	10	0.0000273-0.01	1
7-25	8	45-123	3	Sand clay loam	3	2-4	9	0.01-0.03	2
25-50	5	123-224	6	Sand	4	4-8	8	0.03-0.1	4
50-100	3	224-258	8	Loamy sand	5	8-12	5	0.1-0.3	6
100-250	2			Loam	6	12-18	3	0.3-1.369	10
>250	1			Clay/Silty clay	7	>18	1		
				Clay loam/Sily clay loam/Silt loam	9				

Table A2-Rating of the A and I parameters (Aller et al., 1987).

Lithology classes	Hydrolithology classes	Bedrock material	A and I Rating
Unconsolidated sediments	Unconsolidated	Clay, Gravel, and sand	8
Siliciclastic sediments	Siliciclastic sedimentary	Sandstone, conglomerate	6
Mixed sedimentary rocks	Carbonate	Karst limestone, marly limestone, some dolomites	10
Carbonate sedimentary rocks			
Evaporites			
Basic volcanic rocks	Volcanic	Permeable basalt	9
Acid plutonic rocks	Crystalline	Igneous/metamorphic rocks	A (3), I (4)
Basic plutonic rocks			

Table A3- Land use type and Population Density rating

Land Use Type	Rating	Population Density (people/km^2)	Rating
Urban	8	0-50	1
Croplands	10	50-100	2
Grassland\shrubland	4	100-150	3
Tree\Forest	1	150-200	4
Water Bodies	3	200-250	5
Bare Areas	1	250-300	6
		300-350	7
		350-400	8
		400-450	9
		>450	10